Quasiparticle Dynamics in a Superconducting Qubit Irradiated by a Localized Infrared Source

R. Benevides,[1,2,*] M. Drimmer,[1,2,*] G. Bisson,[1,2] F. Adinolfi,[1,2] U. v. Lüpke,[1,2] H. M. Doeleman,[1,2] G. Catelani,[3,4] and Y. Chu[1,2]

[1]Department of Physics, ETH Zürich, 8093 Zürich, Switzerland
[2]Quantum Center, ETH Zürich, 8093 Zürich, Switzerland
[3]Jülich Aachen Research Alliance (JARA) Institute for Quantum Information (PGI-11), Forschungszentrum Jülich, Jülich 52425, Germany
[4]Quantum Research Center, Technology Innovation Institute, Abu Dhabi 9639, United Arab Emirates

(Received 12 December 2023; accepted 10 July 2024; published 7 August 2024)

A known source of decoherence in superconducting qubits is the presence of broken Cooper pairs, or quasiparticles. These can be generated by high-energy radiation, either present in the environment or purposefully introduced, as in the case of some hybrid quantum devices. Here, we systematically study the properties of a transmon qubit under illumination by focused infrared radiation with various powers, durations, and spatial locations. Despite the high energy of incident photons, our observations agree well with a model of low-energy quasiparticle dynamics dominated by trapping. This technique can be used for understanding and potentially mitigating the effects of high-energy radiation on superconducting circuits with a variety of geometries and materials.

DOI: 10.1103/PhysRevLett.133.060602

The quantum coherence of superconducting (SC) circuits has steadily improved in recent years [1–4]. This has enabled them to not only become one of the leading quantum information processing platforms but also a crucial ingredient in a variety of hybrid devices aiming to combine superconducting circuits with other quantum systems [5,6]. However, understanding and mitigating the sources of decoherence in SC circuits is still an important effort in this field, particularly when considering hybrid systems where new components and degrees of freedom are introduced.

One significant decoherence mechanism is the breaking of Cooper pairs in the superconductor, creating so-called *quasiparticles* [7–9]. The presence of quasiparticles can lead to both energy relaxation and dephasing of qubits [10–16]. These effects were studied using controlled injection of quasiparticles near Josephson junctions with microwave drives [17,18]. It has also been shown that quasiparticles generated by high-energy particles, such as high-energy photons or the products of radioactive decay [19], can even result in correlated errors between multiple qubits [20–24], which is especially detrimental for quantum error correction protocols [25]. To mitigate these detrimental effects, previous studies have focused on shielding SC circuits from environmental high-energy radiation [19,26–28]. However, quasiparticle densities measured are still orders of magnitude higher than predicted at thermal equilibrium [29,30]. In addition, hybrid devices such as microwave-optical quantum transducers require the introduction of a large number of optical photons near SC circuits, which can lead to significant additional decoherence [6,31–33].

In this work, we introduce high-energy radiation in the form of an infrared laser beam in the vicinity of a SC qubit to systematically investigate the impact of incident photons on qubit properties. We vary not only the power and duration but also the location of the laser beam relative to the qubit, demonstrating temporal and spatial control over the generation of quasiparticles. We show that the qubit's excited state lifetime is modified by the incident light, but recovers about an order of magnitude faster than in previous experiments with microwave induced quasiparticles in a similar device [17]. We find that the recovery dynamics of the qubit coherence are well described by a model of quasiparticle population decay through trapping and recombination [17].

Experimental design—Our device consists of an aluminum transmon qubit on a sapphire substrate [1] situated in a 3D aluminum microwave cavity at the base plate of a dilution refrigerator operating around 10 mK. Holes in the walls of the cavity allow laser light to enter and exit the cavity, as seen in Fig. 1(a). Light from a 1550-nm-wavelength laser is guided into the dilution refrigerator via an

*These authors contributed equally to this letter.

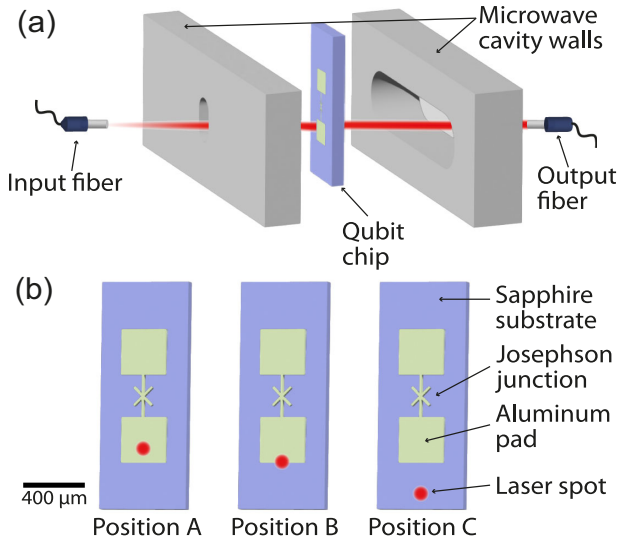

FIG. 1. Schematic of the setup. (a) An infrared laser beam enters its microwave cavity via holes in the walls, reaching the qubit chip. Transmitted light is sent to a collimator (output fiber) and used to construct a low-resolution picture of the qubit. (b) Diagram of the three positions of the laser beam used in this work, labeled A, B, and C. The aluminum pads, as well as the laser spot size and relative locations, are roughly to scale.

optical fiber and focused into the cavity to a beam waist of 47 μm at the plane of the qubit. Variable optical attenuators (VOAs) and a fiber-coupled acousto-optic modulator (AOM) are used to control the power and duration of the laser pulses. At the base plate of the dilution refrigerator, the fiber is glued to an input lens and mounted on a motorized tip-tilt stage that allows us to change the position of the laser spot. A fiber coupler is used to collect the light that exits on the other side of the cavity. By changing the position of the laser beam and measuring the transmitted light, we can take low-resolution images that we use to position the laser beam relative to the qubit (see Supplemental Material [34], Secs. C and D).

We performed measurements with the laser beam focused onto three different locations during a single cooldown, as shown in Fig. 1(b): Position A is on the aluminum pad of the qubit, position B is on the edge of the qubit pad, and position C is on the sapphire substrate, approximately 200 μm below the qubit.

The energy of infrared photons ($\sim h \times 193.4$ THz) is orders of magnitude larger than the superconducting band gap 2Δ of aluminum ($\Delta = h \times 46.9$ GHz, for thin-film aluminum [1]). An infrared photon impinging on the device creates high-energy excitations in the superconducting film and substrate, which are converted into a large number of low-energy quasiparticles through a cascading microscopic process consisting of scattering interactions involving phonons, electrons, and other quasiparticles [40]. The number of low-energy quasiparticles then decreases over time due to two main processes: First, quasiparticles can be individually trapped at the edges of the superconductor or in vortices caused by residual magnetic fields. Second, these electronic excitations can recombine into Cooper pairs, releasing their energy mostly via phonon creation and returning to the superconducting condensate [41].

The light-induced quasiparticle density in the vicinity of the transmon's Josephson junction $x_{\mathrm{qp}}^{\mathrm{in}}$ can be directly inferred from the measured decay rate Γ of the transmon's excited state via $\Gamma = C x_{\mathrm{qp}}^{\mathrm{in}} + \Gamma_0$. Here $C = \sqrt{2\omega_{\mathrm{q}}\Delta/\pi^2\hbar}$, where ω_{q} is the frequency of the qubit transition and Δ is the superconducting energy gap [10]. Γ_0 is the intrinsic decay rate of the qubit in the absence of laser light, which can be due to a constant background quasiparticle density in the material or other sources of decay such as dielectric loss. In our experiment, we measure the qubit energy relaxation time $T_1 = 1/\Gamma$, from which we extract $x_{\mathrm{qp}}^{\mathrm{in}}$ using $C \approx 2\pi \times 7.74$ GHz and Γ_0 measured in the absence of laser light. Measurements using a continuous wave (cw) laser allow us to observe the effect of absorbed light on the steady-state quasiparticle density, while measurements using a laser pulse allow us to study the recovery dynamics of T_1 over the timescales in which quasiparticles are trapped or recombine [17].

Results—Using the cw laser, we find that an increase in the laser power P_{opt} incident on the qubit leads to a shorter T_1, as shown in Fig. 2(a). The data are fitted to a model where the light-induced quasiparticle density depends linearly on the optical power, i.e., $x_{\mathrm{qp}}^{\mathrm{in}} = \mu P_{\mathrm{opt}}$, with μ being a conversion constant between optical power and quasiparticle density. We provide more information about our model in Sec. B of the Supplemental Material [34].

We perform this measurement with the laser located in positions A, B, and C and find a hierarchy of conversion constants given by $\mu_{\mathrm{B}} = (1.61 \pm 0.06) \times 10^{-5}$ nW^{-1} > $\mu_{\mathrm{A}} = (1.75 \pm 0.09) \times 10^{-6}$ nW^{-1} > $\mu_{\mathrm{C}} = (2.96 \pm 0.07) \times 10^{-8}$ nW^{-1}. Position C is the least sensitive to the optical power, which is unsurprising since the laser is focused on the substrate. While most of the light passes through or is specularly reflected at the sapphire-air interfaces and exits through the cavity holes, some diffusely scattered light can remain in the cavity and eventually impinge on the qubit. The T_1 measurements at position A show a higher sensitivity to the optical power than at position C because we are shining the light directly onto the superconducting film. The reflectivity of the Al film at 1550 nm is 97.5% [42], so we believe that most of the light is reflected backwards and leaves the qubit environment through the input hole of the cavity. Surprisingly, we find that when the laser is focused at the edge of the qubit (position B), T_1 is more sensitive to laser power than the other two cases. We speculate that this is because light incident at the border of the qubit diffracts, leading to more photons scattered toward the qubit or remaining in the 3D cavity instead of exiting through the holes. A second possibility would be

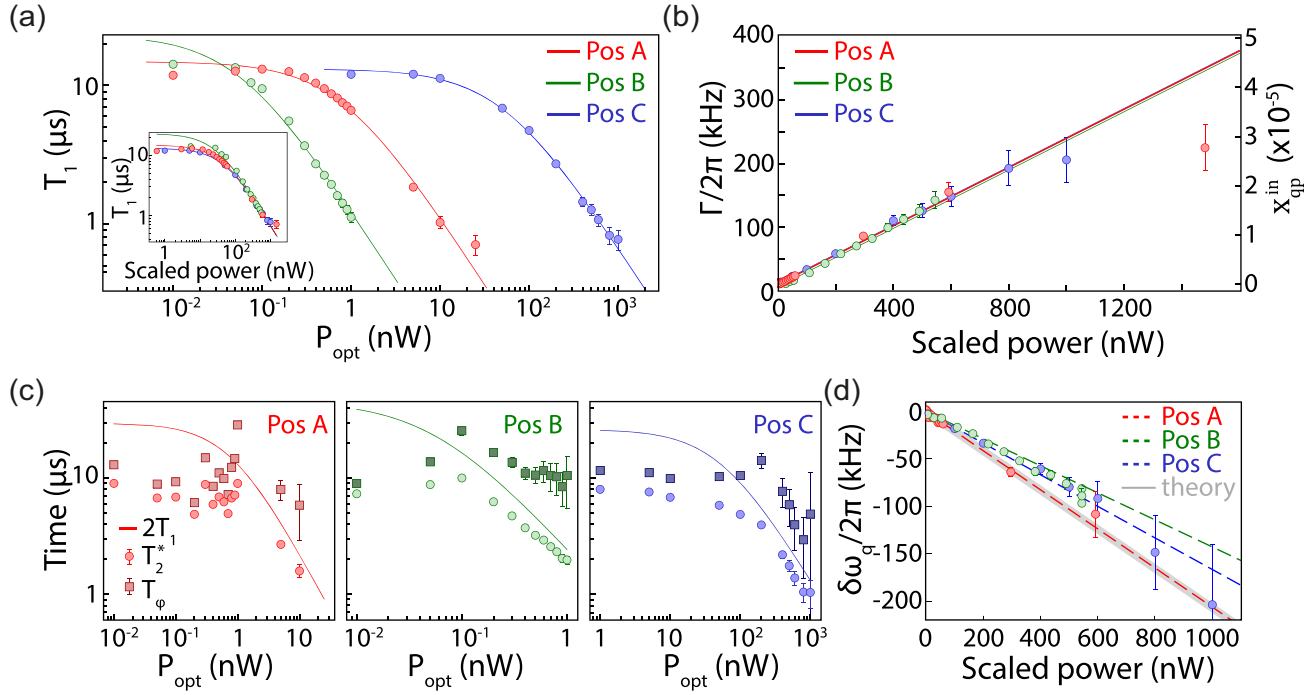

FIG. 2. Measurements with cw laser radiation. (a) T_1 times as a function of laser power, for positions A, B, and C. Inset: The same data with scaled power axes. The power axes are scaled for positions A and B by the ratios $\mu_A/\mu_C \approx 59$ and $\mu_B/\mu_C \approx 544$, respectively. (b) Decay rate of the qubit and the corresponding calculated induced quasiparticle density as a function of power for the laser in positions A, B, and C, illustrating the linear dependence of Γ with the optical power. Power axes of positions A and B are scaled by the same ratios as in (a). (c) Ramsey measurement of the decoherence time (circles), $2T_1$ (solid line), and inferred dephasing time (squares), for the three different positions. (d) Shift of the qubit frequency from its value with the laser turned off. The power axes are again scaled for positions A and B, using the same ratios as in (a). In (a) and (d), the error bars for each data point represent the standard deviation of ten sequential measurements taken at each optical power; in (b) the error bars are propagated from data in (a); in (c), the error bars are calculated using ten sequential measurements and propagation of the error bars in (a).

that photons absorbed in the substrate generate phonons, which lead to the creation of quasiparticles once they travel to the superconductor [25,43]. If this process is more efficient at generating quasiparticles than light directly incident on the superconductor, but it falls off as a function of distance that the phonons have to travel, this would be consistent with our observations. Finally, additional effects at the edges, such as stronger absorption of photons due to fabrication imperfections or local modifications of the superconducting energy gap could also help to explain the higher sensitivity observed with the laser in position B. As can be seen in Fig. 2(b), the qubit decay rate and inferred $x_{\mathrm{qp}}^{\mathrm{in}}$ have a linear dependence on the laser power for the three positions, and therefore all three datasets can be collapsed onto a universal curve when the incident power is scaled by the appropriate ratio of photon-quasiparticle conversion constants.

Quasiparticles have already been demonstrated as an important source of qubit decay and decoherence [12,19]. Here we decompose the quasiparticle-induced decoherence of the qubit into contributions from dephasing and energy decay. In Fig. 2(c), we show the effect of light-induced quasiparticles on the T_2^* decoherence times of our qubit, which decreases with higher optical powers. We can separate the decoherence into two contributions via $1/T_2^* = 1/T_\phi + 1/(2T_1)$, where T_ϕ is the pure dephasing time. We see that while the T_2^* is not T_1 limited for smaller powers, it becomes more so for higher powers. We don't observe statistically significant changes in the T_ϕ of the qubit. This indicates that at high powers, the T_2^* becomes increasingly limited by energy relaxation rather than quasiparticle dephasing. The latter, in contrast to relaxation and frequency shift (discussed next), is in general not determined solely by the quasiparticle density [13]. In this reference, a model considering quasi-thermal equilibrium energy distribution with an effective temperature for the quasiparticles predicts a negligible pure dephasing rate, which is consistent with our measurements.

Finally, from the Ramsey measurements, we also extract the quasiparticle-induced qubit frequency shift, $\delta\omega_q$, as a function of the optical power. Figure 2(d) shows a reduction in the qubit frequency with higher powers. As described in [10], this is another indication of an increased quasiparticle density. We observe that the frequency shift is negative and linear in the optical power applied, as one would expect from a model of quasiparticle injection [see Eq. (73) of

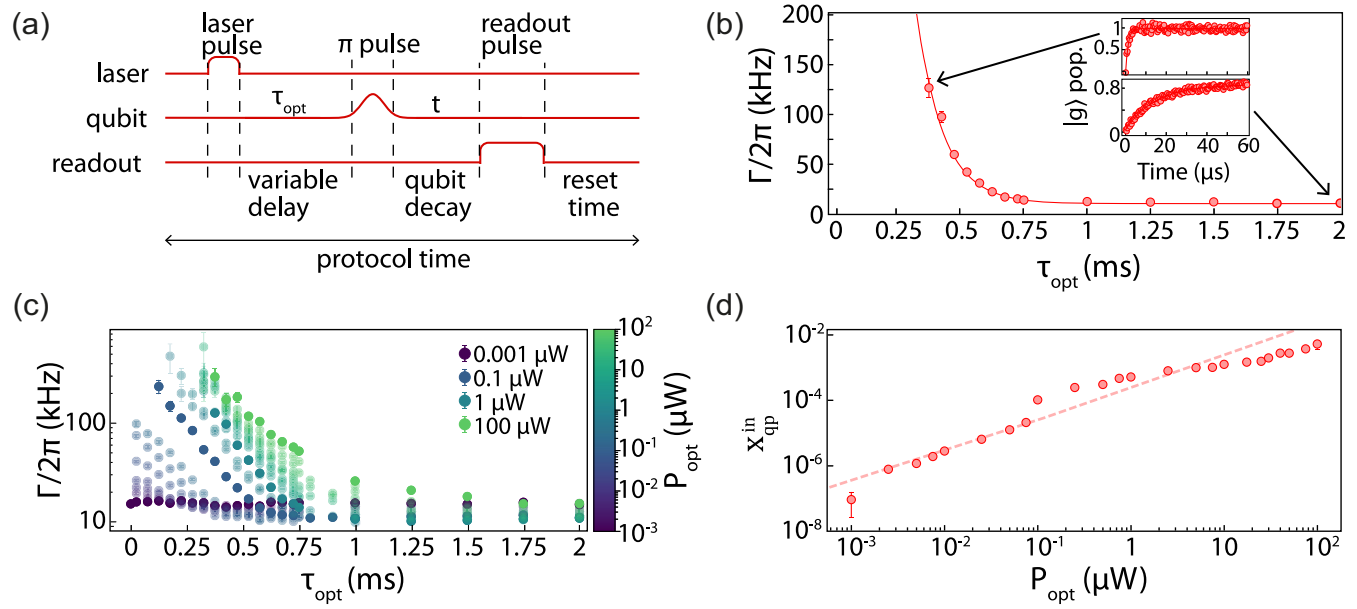

FIG. 3. Time-resolved measurements at position A. (a) Protocol for measurement of qubit T_1 after a laser pulse. (b) Measurement of the qubit decay rate as a function of variable delay time τ_{opt}. Here, we use a 10 μs long laser pulse with an optical power of 1 μW. Insets: Qubit ground state population as a function of time for two different τ_{opt}. (c) Qubit decay rate as a function of τ_{opt} for different optical powers. The data for four powers that span five orders of magnitude are highlighted. (d) Initial injected quasiparticle density $x_{\mathrm{qp}}^{\mathrm{in}}$ as a function of pulse power, obtained from fitting the data in (c). The dashed line is a linear fit to the data where $P_{\mathrm{opt}} \leq 0.1$ μW. Error bars in (b) and (c) represent the standard deviation of measurements, while in (d), they represent the propagated error using our model and the estimated trapping and recombination constants.

Ref. [10]]. Our linear fits in Fig. 2(d) yield slopes which are on average $17\% \pm 6\%$ smaller in absolute value than those expected from theory, when we convert the optical powers to quasiparticle densities. Deviations from the model of this magnitude have been previously observed in Ref. [17]. Based on the results of [44], the smaller slopes could be indicative of quasiparticle heating, but it should be noted that the regime considered there—resonators with a high number of photons below the bandgap—is quite different from the one explored in this work.

Next, we study the recovery of qubit lifetime after quasiparticle creation. In Fig. 3(a), we show the protocol we use for this experiment. The AOM creates laser pulses with controllable pulse lengths and repetition rates. After the pulse is sent to the qubit, we wait a variable delay time τ_{opt} and perform a T_1 measurement.

A typical measurement result is shown in Fig. 3(b). We focus on data for the laser located at position A, but similar results are obtained for the laser in the other positions (see Supplemental Material Sec. H). In the first hundreds of microseconds, we cannot measure the qubit decay rate for higher powers, due to short T_1 times [33]. After a certain time that depends on the pulse energy, we are able to measure a T_1 decay curve, as we show in the inset for the first point in Fig. 3(b). Afterward, we observe a continuous decrease in Γ until it reaches an asymptote at Γ_0.

We perform this experiment for a range of optical powers while keeping the optical pulse length fixed at 10 μs. In Fig. 3(c), we show data for a range of five orders of magnitude in the incident optical power. All plots follow a similar behavior, with an initial higher Γ, followed by a decline that lasts between a few hundred microseconds to slightly more than 1 ms. To understand the physical origin of the coherence recovery, we fit the data for each power to a model that includes trapping and recombination as possible sources of quasiparticle density decrease. Detailed analysis of the fitting parameters leads us to conclude that we can use a model with a quasiparticle trapping constant of $s = 9 \pm 2$ kHz and no recombination, as discussed in Secs. B and I of the Supplemental Material [34]. This allows us to conclude that we are in a trapping-dominated regime, leading to an exponential recovery of the qubit decay rate

$$\Gamma(\tau_{\mathrm{opt}}) = C x_{\mathrm{qp}}^{\mathrm{in}} e^{-s\tau_{\mathrm{opt}}} + \Gamma_0, \tag{1}$$

as we observe in Fig. 3(b). We use this model to extract the injected quasiparticle density at $\tau_{\mathrm{opt}} = 0$ for each laser power, as shown in Fig. 3(d), where we see a clear increase in $x_{\mathrm{qp}}^{\mathrm{in}}$ with optical power. Both the optical power and $x_{\mathrm{qp}}^{\mathrm{in}}$ span 5 orders of magnitude, with the latter reaching values as high as 10^{-2}. We note that similar behavior is observed when varying the pulse length instead of power (Supplemental Material Sec. G [34]).

Discussion and conclusion—In this work, we introduced a technique to create and control quasiparticle dynamics in

SC devices. Using an infrared laser, we were able to tune the qubit decay and decoherence rates by changing the optical energy reaching the device. The increase in the decay rate is directly associated with energy exchange between qubit states and quasiparticle degrees of freedom, which dominates over the dephasing rate.

We believe that the strong laser location dependence observed in our experiment is a combination of two effects: quasiparticle generation due to photons directly absorbed by the SC layer and quasiparticle generation due to photons absorbed in the substrate. In our experiment, we were not able to distinguish between these two processes. However, finding a way to measure the relative strength of these loss mechanisms could be the focus of future investigations. A better understanding of light-induced quasiparticle generation is particularly important for the development of microwave-to-optical transducers based on SC qubits, where one often needs to bring light very close to the superconductors [31,32]. It is also important to stress that a simple linear model of the absorption of photons, using a conversion constant between optical power and quasiparticle density, allows us to precisely describe the results of our cw experiments. This model could be extended by including higher energy levels of the transmon, which in our model is treated like a two-level system.

While the cw dynamics can be explained by a linear absorption model, the pulsed regime shows more complex dynamics. Nonetheless, using a diffusion-free model with power-independent trapping and recombination rates, we were able to fit all of our results and demonstrate how the injected quasiparticle density depends on the pulse energy. We observe that the qubit coherence recovers with a timescale of $\tau_{qp} = 0.11 \pm 0.02$ ms, about one order of magnitude faster than previously reported in an experiment with a similar qubit which used microwave pulses for quasiparticle injection [17]. This could be explained by larger stray magnetic fields resulting in more vortices, faster diffusion due to the higher initial quasiparticle energy, or an altered quasiparticle mean free path.

We believe the platform we have developed can be particularly useful to understand *catastrophic* events associated with cosmic rays or environmental radiation in large-scale SC circuits [21]. With the precise control of power, event rate, and location of the events, we can simulate the burst of injected particles in these circuits and evaluate the robustness of a particular circuit to these events. Finally, in future experiments, *in situ* control of quasiparticle generation could also be used to study quasiparticle diffusion in SC circuits, contributing to our understanding of how to mitigate their detrimental effects.

Acknowledgments—We thank L. Glazman, A. Grimm, Y. Yang, M. Bild, and T. Schatteburg for valuable discussions. This project has received funding from the European Research Council (ERC) under the European Union's Horizon 2020 research and innovation programme (Grant agreement No. 948047). This work was supported by an ETH Zurich Postdoctoral Fellowship. G. C. acknowledges partial support by the U.S. Government under ARO Grant No. W911NF2210257. H. M. D. was supported by a Rubicon grant (Project No. 019.193EN.011) by the Dutch Research Council (NWO) for the duration of this project.

Data availability—All data and software are deposited on Zenodo [45].

U. v. L. fabricated the device. R. B., M. D., G. B., and F. A. constructed the setup. R. B. and M. D. performed the measurements and analyzed the data. R. B., M. D., H. M. D., G. C., and Y. C. interpreted the results. R. B., M. D., and Y. C. conceived the experiment. Y. C. supervised the work. R. B., M. D., and Y. C. wrote the manuscript, which was revised by all authors.

[1] H. Paik, D. I. Schuster, L. S. Bishop, G. Kirchmair, G. Catelani, A. P. Sears, B. R. Johnson, M. J. Reagor, L. Frunzio, L. I. Glazman, S. M. Girvin, M. H. Devoret, and R. J. Schoelkopf, Observation of high coherence in josephson junction qubits measured in a three-dimensional circuit QED architecture, Phys. Rev. Lett. **107**, 240501 (2011).

[2] I. Siddiqi, Engineering high-coherence superconducting qubits, Nat. Rev. Mater. **6**, 875 (2021).

[3] A. P. M. Place, L. V. H. Rodgers, P. Mundada, B. M. Smitham, M. Fitzpatrick, Z. Leng, A. Premkumar, J. Bryon, A. Vrajitoarea, S. Sussman, G. Cheng, T. Madhavan, H. K. Babla, X. H. Le, Y. Gang, B. Jäck, A. Gyenis, N. Yao, R. J. Cava, N. P. de Leon, and A. A. Houck, New material platform for superconducting transmon qubits with coherence times exceeding 0.3 milliseconds, Nat. Commun. **12**, 1779 (2021).

[4] S. Ganjam, Y. Wang, Y. Lu, A. Banerjee, C. U. Lei, L. Krayzman, K. Kisslinger, C. Zhou, R. Li, Y. Jia, M. Liu, L. Frunzio, and R. J. Schoelkopf, Surpassing millisecond coherence times in on-chip superconducting quantum memories by optimizing materials, processes, and circuit design, Nat. Commun. **15**, 3687 (2024).

[5] A. Clerk, K. Lehnert, P. Bertet, J. Petta, and Y. Nakamura, Hybrid quantum systems with circuit quantum electrodynamics, Nat. Phys. **16**, 257 (2020).

[6] Y. Chu and S. Gröblacher, A perspective on hybrid quantum opto- and electromechanical systems, Appl. Phys. Lett. **117**, 150503 (2020).

[7] L. I. Glazman and G. Catelani, Bogoliubov quasiparticles in superconducting qubits, SciPost Phys. Lect. Notes 31 (2021).

[8] K. Y. Arutyunov, S. A. Chernyaev, T. Karabassov, D. S. Lvov, V. S. Stolyarov, and A. S. Vasenko, Relaxation of nonequilibrium quasiparticles in mesoscopic size superconductors, J. Phys. Condens. Matter **30**, 343001 (2018).

[9] P. J. de Visser, J. J. A. Baselmans, P. Diener, S. J. C. Yates, A. Endo, and T. M. Klapwijk, Number fluctuations of sparse quasiparticles in a superconductor, Phys. Rev. Lett. **106**, 167004 (2011).

[10] G. Catelani, R. J. Schoelkopf, M. H. Devoret, and L. I. Glazman, Relaxation and frequency shifts induced by quasiparticles in superconducting qubits, Phys. Rev. B **84**, 064517 (2011).
[11] J. M. Martinis, M. Ansmann, and J. Aumentado, Energy decay in superconducting Josephson-junction qubits from nonequilibrium quasiparticle excitations, Phys. Rev. Lett. **103**, 097002 (2009).
[12] M. Lenander, H. Wang, R. C. Bialczak, E. Lucero, M. Mariantoni, M. Neeley, A. O'Connell, D. Sank, M. Weides, J. Wenner *et al.*, Measurement of energy decay in superconducting qubits from nonequilibrium quasiparticles, Phys. Rev. B **84**, 024501 (2011).
[13] G. Catelani, S. E. Nigg, S. M. Girvin, R. J. Schoelkopf, and L. I. Glazman, Decoherence of superconducting qubits caused by quasiparticle tunneling, Phys. Rev. B **86**, 184514 (2012).
[14] J. Aumentado, M. W. Keller, J. M. Martinis, and M. H. Devoret, Nonequilibrium quasiparticles and $2e$ periodicity in single-cooper-pair transistors, Phys. Rev. Lett. **92**, 066802 (2004).
[15] M. D. Shaw, R. M. Lutchyn, P. Delsing, and P. M. Echternach, Kinetics of nonequilibrium quasiparticle tunneling in superconducting charge qubits, Phys. Rev. B **78**, 024503 (2008).
[16] U. Vool, I. M. Pop, K. Sliwa, B. Abdo, C. Wang, T. Brecht, Y. Y. Gao, S. Shankar, M. Hatridge, G. Catelani, M. Mirrahimi, L. Frunzio, R. J. Schoelkopf, L. I. Glazman, and M. H. Devoret, Non-poissonian quantum jumps of a fluxonium qubit due to quasiparticle excitations, Phys. Rev. Lett. **113**, 247001 (2014).
[17] C. Wang, Y. Y. Gao, I. M. Pop, U. Vool, C. Axline, T. Brecht, R. W. Heeres, L. Frunzio, M. H. Devoret, G. Catelani, L. I. Glazman, and R. J. Schoelkopf, Measurement and control of quasiparticle dynamics in a superconducting qubit, Nat. Commun. **5**, 5836 (2014).
[18] C.-H. Liu, D. C. Harrison, S. Patel, C. D. Wilen, O. Rafferty, A. Shearrow, A. Ballard, V. Iaia, J. Ku, B. L. T. Plourde, and R. McDermott, Quasiparticle poisoning of superconducting qubits from resonant absorption of pair-breaking photons, Phys. Rev. Lett. **132**, 017001 (2024).
[19] A. P. Vepsäläinen, A. H. Karamlou, J. L. Orrell, A. S. Dogra, B. Loer, F. Vasconcelos, D. K. Kim, A. J. Melville, B. M. Niedzielski, J. L. Yoder *et al.*, Impact of ionizing radiation on superconducting qubit coherence, Nature (London) **584**, 551 (2020).
[20] C. D. Wilen, S. Abdullah, N. Kurinsky, C. Stanford, L. Cardani, G. d'Imperio, C. Tomei, L. Faoro, L. Ioffe, C. Liu *et al.*, Correlated charge noise and relaxation errors in superconducting qubits, Nature (London) **594**, 369 (2021).
[21] M. McEwen *et al.*, Resolving catastrophic error bursts from cosmic rays in large arrays of superconducting qubits, Nat. Phys. **18**, 107 (2022).
[22] P. M. Harrington, M. Li, M. Hays, W. V. D. Pontseele, D. Mayer, H. D. Pinckney, F. Contipelli, M. Gingras, B. M. Niedzielski, H. Stickler, J. L. Yoder, M. E. Schwartz, J. A. Grover, K. Serniak, W. D. Oliver, and J. A. Formaggio, Synchronous detection of cosmic rays and correlated errors in superconducting qubit arrays, arXiv:2402.03208.
[23] X.-G. Li, J.-H. Wang, Y.-Y. Jiang, G.-M. Xue, X.-X. Cai, J. Zhou, M. Gong, Z.-F. Liu, S.-Y. Zheng, D.-K. Ma, M. Chen, W.-J. Sun, S. Yang, F. Yan, Y.-R. Jin, X.-F. Ding, and H.-F. Yu, Direct evidence for cosmic-ray-induced correlated errors in superconducting qubit array, arXiv:2402.04245.
[24] M. McEwen *et al.*, Resisting high-energy impact events through gap engineering in superconducting qubit arrays, arXiv:2402.15644.
[25] J. M. Martinis, Saving superconducting quantum processors from decay and correlated errors generated by gamma and cosmic rays, npj Quantum Inf. **7**, 90 (2021).
[26] A. D. Córcoles, J. M. Chow, J. M. Gambetta, C. Rigetti, J. R. Rozen, G. A. Keefe, M. Beth Rothwell, M. B. Ketchen, and M. Steffen, Protecting superconducting qubits from radiation, Appl. Phys. Lett. **99**, 181906 (2011).
[27] R. Barends, J. Wenner, M. Lenander, Y. Chen, R. C. Bialczak, J. Kelly, E. Lucero, P. O'Malley, M. Mariantoni, D. Sank, H. Wang, T. C. White, Y. Yin, J. Zhao, A. N. Cleland, J. M. Martinis, and J. J. Baselmans, Minimizing quasiparticle generation from stray infrared light in superconducting quantum circuits, Appl. Phys. Lett. **99**, 113507 (2011).
[28] L. Cardani, F. Valenti, N. Casali, G. Catelani, T. Charpentier, M. Clemenza, I. Colantoni, A. Cruciani, G. D'Imperio, L. Gironi *et al.*, Reducing the impact of radioactivity on quantum circuits in a deep-underground facility, Nat. Commun. **12**, 2733 (2021).
[29] K. Serniak, M. Hays, G. De Lange, S. Diamond, S. Shankar, L. Burkhart, L. Frunzio, M. Houzet, and M. Devoret, Hot nonequilibrium quasiparticles in transmon qubits, Phys. Rev. Lett. **121**, 157701 (2018).
[30] X. Pan, Y. Zhou, H. Yuan, L. Nie, W. Wei, L. Zhang, J. Li, S. Liu, Z. Jiang, G. Catelani, L. Hu, F. Yan, and D. Yu, Engineering superconducting qubits to reduce quasiparticles and charge noise, Nat. Commun. **13**, 7196 (2022).
[31] M. Mirhosseini, A. Sipahigil, M. Kalaee, and O. Painter, Superconducting qubit to optical photon transduction, Nature (London) **588**, 599 (2020).
[32] R. Delaney, M. Urmey, S. Mittal, B. Brubaker, J. Kindem, P. Burns, C. Regal, and K. Lehnert, Superconducting-qubit readout via low-backaction electro-optic transduction, Nature (London) **606**, 489 (2022).
[33] M. Xu, C. Li, Y. Xu, and H. X. Tang, Light-induced microwave noise in superconducting microwave-optical transducers, Phys. Rev. Appl. **21**, 014022 (2024).
[34] See Supplemental Material at http://link.aps.org/supplemental/10.1103/PhysRevLett.133.060602 for details, including (A) Qubit details, (B) modeling the experiment, (C) details of the experimental setup, (D) imaging inside the dilution refrigerator, (E) thermal analysis with finite element methods, (F) measurements of the thermal population of the qubit (G) quasiparticle relaxation as a function of pulse length, (H) pulse energy comparison, and (I) details on data processing, which includes Refs. [35–39].
[35] C. Wang, C. Axline, Y. Y. Gao, T. Brecht, Y. Chu, L. Frunzio, M. H. Devoret, and R. J. Schoelkopf, Surface participation and dielectric loss in superconducting qubits, Appl. Phys. Lett. **107**, 162601 (2015).

[36] M. Houzet, K. Serniak, G. Catelani, M. H. Devoret, and L. I. Glazman, Photon-assisted charge-parity jumps in a superconducting qubit, Phys. Rev. Lett. **123**, 107704 (2019).
[37] A. Rothwarf and B. Taylor, Measurement of recombination lifetimes in superconductors, Phys. Rev. Lett. **19**, 27 (1967).
[38] K. Geerlings, Z. Leghtas, I. M. Pop, S. Shankar, L. Frunzio, R. J. Schoelkopf, M. Mirrahimi, and M. H. Devoret, Demonstrating a driven reset protocol for a superconducting qubit, Phys. Rev. Lett. **110**, 120501 (2013).
[39] F. Pobell, *Matter and Methods at Low Temperatures* (Springer Berlin Heidelberg, Berlin, Heidelberg, 2013).
[40] A. G. Kozorezov, A. F. Volkov, J. K. Wigmore, A. Peacock, A. Poelaert, and R. den Hartog, Quasiparticle-phonon downconversion in nonequilibrium superconductors, Phys. Rev. B **61**, 11807 (2000).
[41] S. B. Kaplan, C. Chi, D. Langenberg, J.-J. Chang, S. Jafarey, and D. Scalapino, Quasiparticle and phonon lifetimes in superconductors, Phys. Rev. B **14**, 4854 (1976).
[42] K. M. McPeak, S. V. Jayanti, S. J. P. Kress, S. Meyer, S. Iotti, A. Rossinelli, and D. J. Norris, Plasmonic films can easily be better: Rules and recipes, ACS Photonics **2**, 326 (2015).
[43] E. Yelton, C. P. Larson, V. Iaia, K. Dodge, G. L. Magna, P. G. Baity, I. V. Pechenezhskiy, R. McDermott, N. Kurinsky, G. Catelani, and B. L. T. Plourde, Modeling phonon-mediated quasiparticle poisoning in superconducting qubit arrays, Phys. Rev. B **110**, 024519 (2024).
[44] P. B. Fischer and G. Catelani, Nonequilibrium quasiparticle distribution in superconducting resonators: An analytical approach, Phys. Rev. Appl. **19**, 054087 (2023).
[45] R. Benevides, M. Drimmer, G. Bisson, F. Adinolfi, U. v. Lupke, H. M. Doeleman, G. Catelani, and Y. Chu, Data and codes for the work: Quasiparticle dynamics in a superconducting qubit irradiated by a localized infrared source (2024), 10.5281/zenodo.11548753.